Commun. Comput. Phys.
doi: 10.4208/cicp.301209.230710a

Vol. **10**, No. 1, pp. 120-139
July 2011

Flow-Induced Acoustics in Corrugated Pipes

Mihaela Popescu[1], Stein Tore Johansen[1] and Wei Shyy[2,*]

[1] *Department of Process Technology, Flow Technology, SINTEF Materials and Chemistry, 7046 Trondheim, Norway.*
[2] *Department of Aerospace Engineering, University of Michigan, Ann Arbor, MI 48109, USA.*

Received 30 December 2009; Accepted (in revised version) 23 July 2010

Available online 24 March 2011

Abstract. When gas flows through corrugated pipes, pressure waves interacting with vortex shedding can produce distinct tonal noise and structural vibration. Based on established observations, a model is proposed which couples an acoustic pipe and self-excited oscillations with vortex shedding over the corrugation cavities. In the model, the acoustic response of the corrugated pipe is simulated by connecting the lossless medium moving with a constant velocity with a source based on a discrete distribution of van der Pol oscillators arranged along the pipe. Our time accurate solutions exhibit dynamic behavior consistent with that experimentally observed, including the lock-in frequency of vortex shedding, standing waves and the onset fluid velocity capable of generating the lock-in.

AMS subject classifications: 76Q05

Key words: Computational fluid dynamics, aeroacoustics, sound generation, riser, corrugated pipes, wave propagation, low Mach number, gas flow, flow-induced vibrations.

1 Introduction

Flexible risers are specially designed pipes that facilitate fluid flow between sea installations and surface facilities located on drill platforms (see Fig. 1). The flexible risers often experience the phenomenon of "singing": large pressure fluctuations are generated within the riser and can be heard clearly as acoustic tones. The problem can be attributed to flow induced pulsations that are generated on the inner corrugated wall layer of the flexible riser. When the vortex shedding frequency excites the acoustic natural frequency of the pipeline, resonance between structural vibrations, standing acoustical waves and vortex shedding appear. This phenomenon is known as lock-in. The minimum fluid velocity for which a lock-in frequency appears is referred to as the onset velocity.

*Corresponding author. *Email addresses:* mihaela.popescu@sintef.no (M. Popescu), stein.t.johansen@sintef.no (S. T. Johansen), weishyy@umich.edu (W. Shyy)

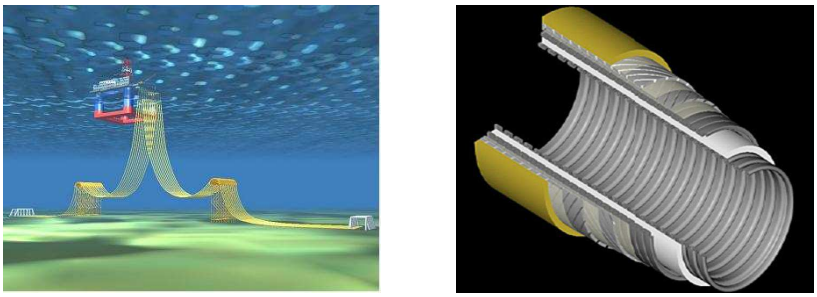

(a) (b)

Figure 1: Flexible riser: (a) General view of offshore flexible riser system; (b) The structure of flexible riser.

Various studies have been conducted to better understand the vortex shedding and acoustics associated with flows in corrugated pipes. The shedding frequency of vortices can be characterized by the Strouhal number, defined as $S_t = f \cdot L/U$, where f is the frequency, L is characteristic length and U is characteristic velocity. Ziada et al. [33] established that the vibrations occur over a certain range of Strouhal numbers. Nakamura and Fukamachi [20] showed that the frequency of the loudest sound from a corrugated pipe is proportional to the flow velocity. In other words, the Strouhal number can be approximated as constant. Weaver and Ainsworth [32] showed that the Strouhal number is typically larger than 0.45 for the maximum vibration amplitude. This value is in agreement with the results of Gerlach [10], Bass and Holster [2] and Klaeui [17]. Furthermore, Nakamura and Fukamachi [20], and Kristiansen and Wiik [19] reported the connection between sound emitted in a tube and shear layer instability resulting from the flow over the corrugation. They suggested that the interaction between the fluid flow and the cavities is responsible for the resonance and noise. In a more generic context, Howe [14] demonstrated theoretically that shear layer-cavity interaction results in two types of resonance sources: monopole and dipole. Hémon et al. [12] presented an experimental and theoretical study of the pressure oscillations generated by the flow over a deep cavity. A review of recent advances in understanding, modeling and controlling oscillations of flow past a cavity has been given by Rowley and Williams [28].

Rockwell and Schachenmann [25] provided the first measurements of the physical behavior of an unsteady shear layer along the mouth of a circular cavity at the end of a long pipe, including both the locked-in and the non-locked-in state. They showed that during lock-in, the magnitude of the fluctuating velocity due to acoustic resonance is within the same order as that associated with the hydrodynamic fluctuations.

There is also work done specifically in modeling of the fluid flow over cavities. Debut et al. [6,7] presented a phenomenological model of the flow around a corrugation. They proposed a way to describe the feedback mechanism of the acoustics-cavity interactions. Unfortunately, this model describes the flow from the middle of the pipe like a collection of discrete sources. Tam and Block [29] derived a mathematical model of an acoustic cavity, and explored coupling of cavity tones, shear layer instability and acoustic feedback

to help understand the tone generation mechanism. An important contribution by this model is the inclusion of the shear layer thickness.

The purpose of this work is to develop a suitable one-dimensional and transient computational model, capable of capturing the main dynamic characteristics of the feedback mechanism between fluid flows and acoustics. The study was motivated by our interest in investigating vibration problems associated with flexible corrugated risers, while transporting dry gas. We address the coupling mechanism between acoustic oscillations and the fluid flow over a series of cavities. First we present and discuss Navier-Stokes flow computations around a single cavity (of depth 3.11E-03m and the average width 3.12E-03m), as part of a long (6.148E-01m) corrugated pipe involving 116 cavities. The study of flows around a single cavity can not produce all details needed for describing flow oscillations and the corresponding acoustic modes. However, it does provide valuable insight into the aero-acoustic mechanisms in corrugated pipes. Then, we present in detail our one-dimensional mathematical model which includes a coupling mechanism between singing in the corrugated pipe and flow-induced oscillations, caused by vortex shedding. The model is based on a wave equation representing the acoustic field, coupled with self-excited equations of the Van der Pol type, accounting for fluid-induced oscillations around cavities. The aero-acoustic coupling is expressed in terms of a pressure gradient source. The frequency that characterizes the vortex shedding can be determined by computing the flow over a single cavity in the form of the Strouhal number. We assess the outcome of the model via direct experimental comparison, in particular, the lock-in frequency and onset fluid velocity.

2 General description of pipe flows around cavities

As already mentioned, the fundamental cause of the vibrations of a corrugated pipe is the vortex shedding around cavities. The acoustic field and the aerodynamic flow field strongly interact at resonance conditions. The acoustic flow velocity influences the rolling-up process when shed vortices are convected downstream. At the same time the aerodynamic flow field also influences the acoustic flow field: energy is transferred from the former to the latter flow field under specific physical conditions. Identification of these conditions is one of the main objectives of the present paper. The computation of the flow structure and the acoustic pressure level for flow that passes over the cavities can give valuable information about shed vortices. Before considering the coupling between vortex shedding and pressure oscillations, we present initial computations based on the Navier-Stokes equations, to probe some of the basic characteristics of the flow field in such geometries. In these simulations a possible fluid-structure interaction between the vortex shedding and the pipe structure was assumed negligible. The Navier-Stokes computations have been done using the commercial flow code FLUENT 6.3. Based on the insight gained, we will present a one-dimensional flow-acoustics model accounting for the coupling between pressure waves and vortex shedding.

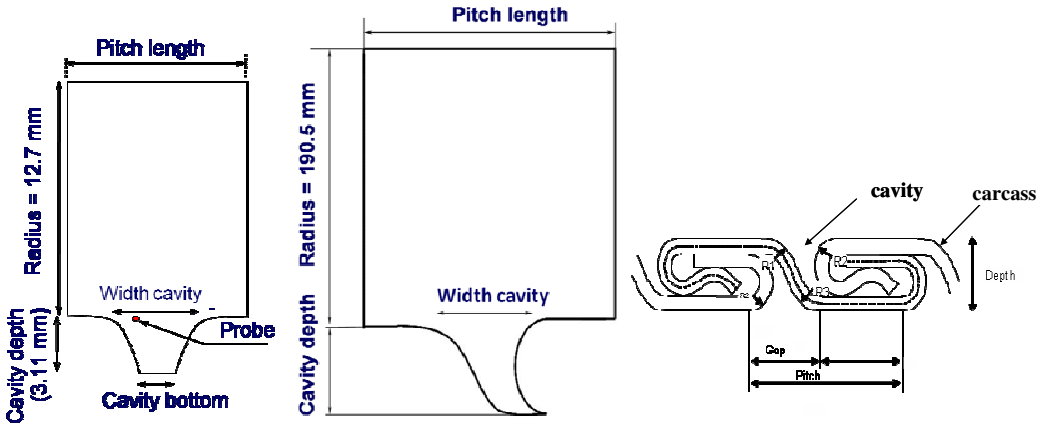

(a) (b) (c)

Figure 2: General description of the corrugation: (a) Case I; (b) Case II; (c) geometrical details of the corrugated pipe (flexible riser), Case II.

2.1 Single cavity flow

Fig. 2(a) shows a general view of the geometry and the dimension of the carcass. The rounded shape of the edges from the top of the cavity was preserved, but the rounded shape of the cavity bottom has been replaced by straight edges because we consider that this has no influence on the flow field. The details of the geometry are important because these parameters influence the characteristics of the vortex shedding: i) inner diameter of the pipe is 2.54E-02m; ii) cavity depth is 3.11E-03m; iii) the average cavity width is 3.12E-03m; iv) cavity pitch length is equal to width of the cavity plus the distance between two neighboring cavities (see Fig. 2).

The computations were done for flow velocities between 8 and 20m/s: i) 2D axisymmetric computations: the symmetry axis of the computations is the axis of the pipe; ii) mass flux periodic condition over a single cavity, which makes the computations equivalent with simulation of the flow in an infinite pipe; iii) compressible computation (to obtain the acoustic details); iv) turbulence model: LES (Smagorinsky model); v) far field density $\rho_0 = 1.225$. The resulting Reynolds number based on pipe diameter is between 1.39E+04 and 3.48E+04.

A probe was introduced in the cavity to capture the fluctuation of the flow inside the cavity. These fluctuations are important because they are the source of the acoustic pipe.

Fig. 3 shows a snapshot of the velocity vectors and pressure around the cavity. This picture illustrates that vortices are born inside or at the edge of the cavity. The pressure distribution clearly shows a high pressure stagnation point in the corner of the cavity and the pulsating vortex line. These travelling and impinging vortices are the source of the acoustic waves that may develop in a corrugated pipe and can sustain powerful waves. However, if the vortex is too weak it cannot trigger a large scale acoustic field and sustain singing.

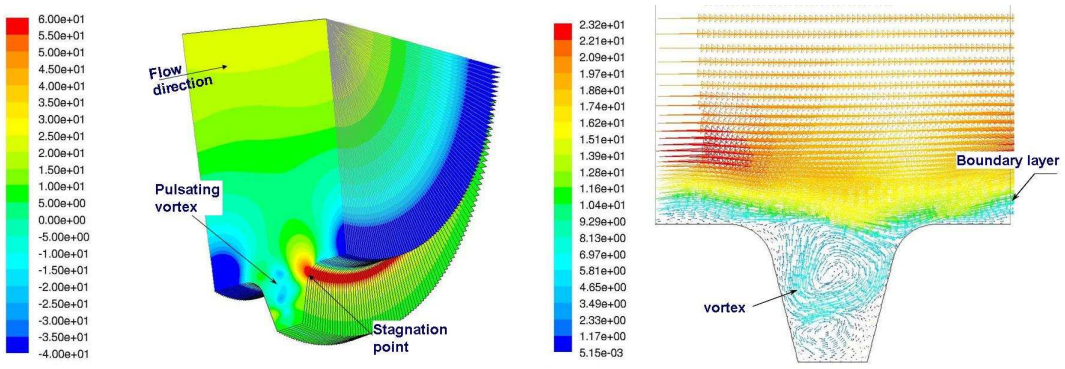

(a) (b)

Figure 3: Flow around 8.0E.03m pitch cavity; inlet velocity $U=18$m/s, $t=0.005$s: (a) pressure distribution; (b) velocity stream line.

The influence of the length of the pitch is analyzed considering two cavities that have the same geometry characteristics, except for the length of the pitch which is 5.3E-03m, respective 8.0E-03m pitch. For these geometries we consider the computation of the flow with an average velocity of 18m/s. We remark that in the case of the longer pitch, the period of interaction between vortices originated in two consecutive cavities is longer than in the shorter pitch cavity case. This explains the change in the frequency of the pressure inside the cavity. The Strouhal number is lower for the cavity with a longer pitch, as we can see in Fig. 4. This demonstrates that the characteristics of the pressure wave, caused by the traveling vortices, are the result of not only the flow and geometry (shape of the cavity) but also the convective speed of the vortex and the interaction period between vortices that are born in different cavities.

The frequency increases with the value of the velocity, explaining why the Strouhal number based on pitch length is almost constant for a given corrugation geometry. Such a linear relationship between frequency and critical velocity was also noticed experimentally by Kristiansen and Wiik [19].

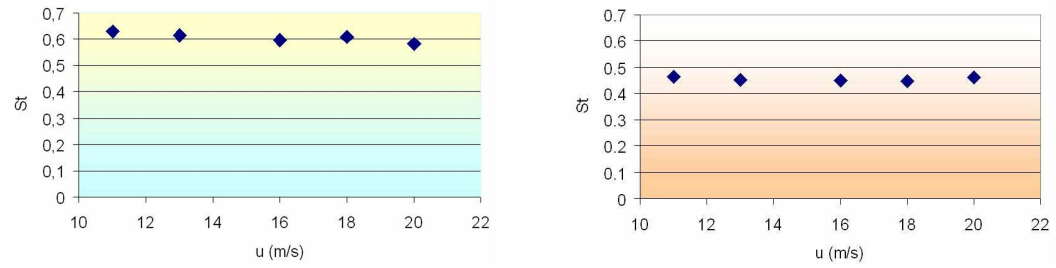

(a) (b)

Figure 4: 2D compressible flow prediction: Strouhal Number for first case geometry-based on pitch length: (a) pitch = 5.3mm; (b) pitch = 8mm.

The computations of the flow around single cavity, using periodic mass flow boundary conditions have two limitations: (i) The lack of a resonance condition; in this case the pipe will not sing easily. However, the computation can indicate if the pipe has singing potential. (ii) Lack of the frequency lock-on mechanism, due to a lack of resonance in the fluid flow model.

However, even though these computations cannot capture all details of the flow around the cavity in the singing condition, they give valuable information about the characteristics of the acoustic pressure wave sources in the corrugated pipe, regarding type of acoustic source and frequency. This insight is exploited to develop the flow-acoustics model presented later in the paper.

2.2 Characterization of the sound field around the cavity

The characterization of the sound is done only for the first 0.02s, where the flow exhibits singing. The directivity was studied in order to measure the radiation pattern of the source. The directional characteristic of a source is described by the amplitude directivity function D, defined as the rms of the acoustic pressure radiated into a direction defined by the angle θ, relative to the rms of the acoustic pressure radiated into the angle where the maximum acoustic pressure rms $\theta_{\max}$ appears:

$$D(\theta) = \frac{p(R,\theta)}{p(R,\theta_{\max})}. \tag{2.1}$$

The pressure p is the rms of the acoustic pressure value, where the mean is over a defined time (0.01s) and at distance R equal to 2m from the origin of sound source, which is the cavity. The directivity indicates how effectively the source concentrates its available acoustic power. The acoustic pressure was recorded in 33 points around the cavity. Fig. 5 shows the directivity for an average velocity of 18m/s: we found that the directivity is a radial dipole.

The dominant frequency for the sound is identical to the fluctuation frequency of the flow pressure in the cavity.

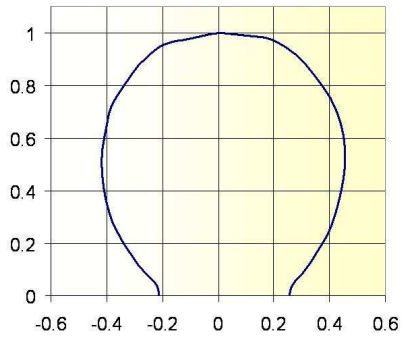

Figure 5: The directive function of the sound generated by the presence of the cavity: radial dipole.

Similar results were obtained for the other average flow velocities between 8m/s to 20m/s: i) the same shape of directivity function; ii) frequency of the sound is the same as the flow pressure in the cavity.

2.3 Flow in a corrugated pipe

The study was done for a pipe with a length of 0.6148m. It has the previously defined corrugation geometry: the corrugation pitch is 5.3E-03m (see Fig. 2(a)). The computational grid was chosen to be sufficiently fine: i) inside cavity grid $\Delta x \approx$ 8.0E-05m; ii) there are nine grid layers around the cavity wall that increase from $\Delta x \approx$ 2.0E-05m (near the wall) to $\Delta x \approx$ 8.0E-05m. The grid was chosen to capture the details of the vortex shedding, which has a direct impact on the generation of the sound signal and the wave profile in the pipe. The corrugated pipe flow computation was based on the same conditions and models as those around a single cavity: i) 2D axisymmetric computation-the symmetry axis of the computation is the axis of the pipe; ii) $M<0.01$; iii) compressible computation; iv) turbulence model: LES (Smagorinsky model); iv) Far field density $\rho_0=1.225$.

Using the model and grid presented above, Popescu and Johansen [21] showed that for cavity flows the maximum shear layer instability is found in the regions with maximum acoustic pressure variations. This indicates how the fluid system is influenced by the acoustic subsystem. The phenomenon can be understood by examining these two subsystems: the acoustic subsystem and the fluid flow subsystem. These two subsystems are strongly coupled in such a way that: i) the acoustic subsystem is driven by the vortex-induced pressure variation; ii) the fluid subsystem is influenced and controlled by the acoustic pressure. Thus, the acoustic oscillations in the corrugated tube are self-excited oscillations occurring in a fluid-acoustic coupled system. The essential feature of the natural frequency of the fluid subsystem is that it is proportional to the velocity of the flow. In consequence the imposed acoustic oscillations can set the fluid subsystem into resonance when the resonance velocity is approached. Here, we present the solution of a corrugated pipe flow of 13m/s in the same geometry and Re=2.26E+04.

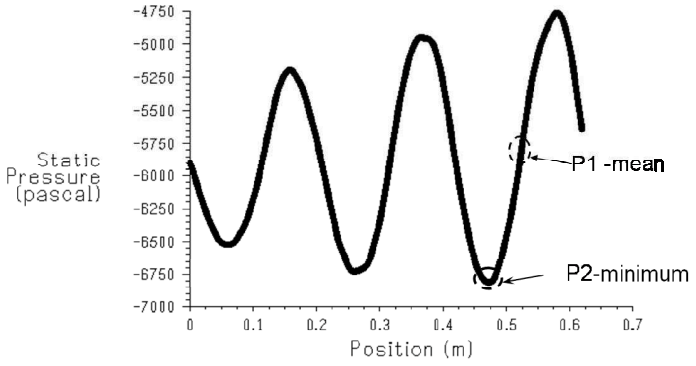

Figure 6: Static pressure [Pa] on the axis of the pipe, $t=0.1907$s, $U=13$m/s.

Fig. 6 shows a snap-shot of the pressure distribution in the centre of the corrugated pipe for the average velocity of U=13m/s, in which we marked points where mean and minimum pressure will be analyzed. In this picture we can see clearly six extreme values (maxima/minima) that correspond to the almost standing wave. Fig. 7(a) shows velocity vector in the area of the pipe where there is an extreme (minimum) of acoustic pressure amplitude. Here we find very well defined pulsating vortices, which will contribute to the acoustic source. Fig. 7(b) shows velocity vectors in the area of the mean acoustic pressure. In this zone, some very weak vortices can be seen. Therefore these mean zones are not expected to significantly influence the large scale of the acoustic field. These two observations emphasize: i) how the fluid and acoustic subsystems influence one each other: acoustic pressure control the pulsating vortex activity, and the vortex is the source for acoustic pressure; ii) acoustic pressure and source flow velocity are in phase.

In case of a standing wave situation, we have pressure maxima that are placed at fixed locations. In these positions, the interaction between acoustic, pressure and shear layers is most powerful and there is a high probability to maintain singing and the standing wave.

The local mechanism between acoustics and flow was well described by Rossiter [27] and Colonius at al. [4]: i) mechanical shear layer instability and growth of vortices in the shear layer; ii) the impingement of the vortices at the downstream cavity edges, and subsequent scattering of acoustic waves; iii) the transmission of acoustic waves upstream and iv) the conversion to radial velocity fluctuations at the cavity leading edge. We have integrated this local mechanism in a large feedback loop where we take into consideration the interaction between flow and acoustics. The feedback mechanism between acoustic subsystem and the fluid subsystem is described by the diagram from Fig. 8.

Numerical studies of the flow in the pipe are done for an average flow speed between 8m/s to 20m/s. These results are compared with solution of the flow around one cavity (periodic boundary condition) and experimental results (see Table 1). Recall that the solution of the flow around a single cavity can not reproduce the lock on frequency, but can approximate the characteristic frequency. This valuable observation will be used in the numerical model approach that we develop in this paper.

Table 1: The characteristics of the acoustics: frequency and Strouhal number computed (for flow around single cavity and 6.148E-01m long pipe) and measured (for 6.148E-01m long pipe).

U[m/s]	Mode Number	Frequency[Hz] (computed -1 cavity)	Frequency[Hz] (measured - pipe)	Frequency[Hz] (computed - pipe)	St (computed -1 cavity)	St (measured - pipe)	St (computed - pipe)
8	4	920	990	980	0.6095	0.65588	0.64925
9.5	5	1100	1230	1275	0.61368	0.68621	0.71132
11	5	1268	1230	1273	0.61095	0.59264	0.61335
13	6	1510	1497	1516	0.61562	0.61032	0.61806
15.6	7	1793	1731	1765	0.60916	0.5881	0.59965
18	8	2070	1968	1978	0.6095	0.57947	0.58241
20	9	2290	2216	2232	0.60685	0.58724	0.59148

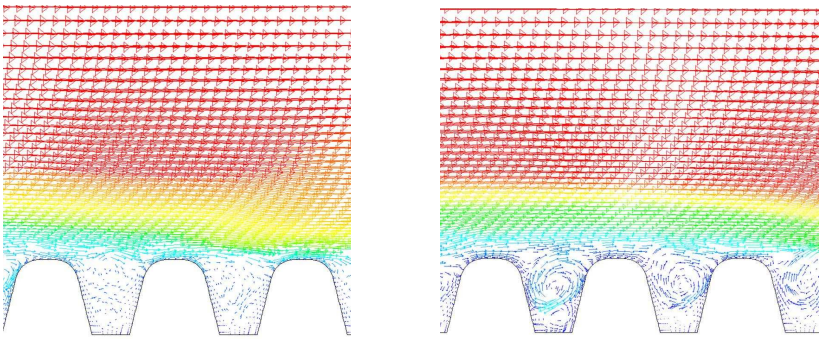

(a) (b)

Figure 7: Vector of velocity t=0.1987s, U=13m/s: (a) velocity vector in the zone of the corrugated pipe where acoustic pressure present a mean value ($P1$ zone); (b) velocity vector in the zone of the corrugated pipe where acoustic pressure present an extreme value ($P2$ zone).

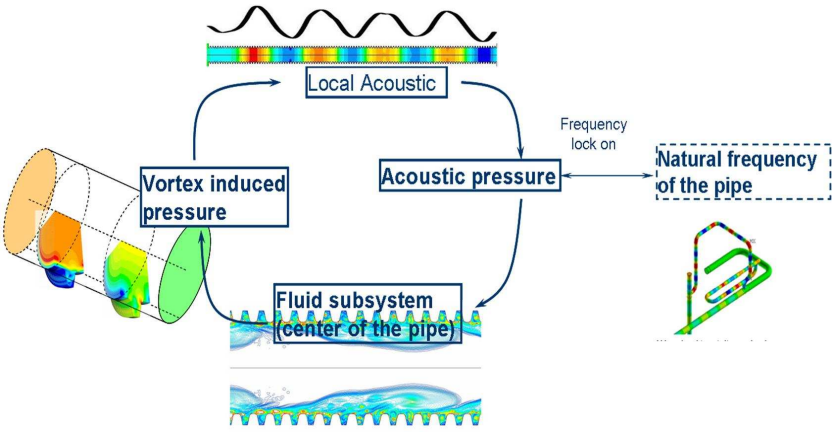

Figure 8: Feedback mechanism between flow and acoustic field.

3 One-dimensional flow-acoustics model

The one dimensional flow-acoustics model consists of two key components: (i) the acoustic pipe, which is driven by the vortex-induced pressure variation; (ii) self-excited oscillators representing the vortex excitation caused by the flow over corrugations, which is controlled by the acoustic pressure.

3.1 Model for pressure in a corrugated pipe

A simple and reasonable model for the standard damped mechanical oscillator excited by the shear layer instability in neck for the Helmholtz resonator is described by the

following equation (Hémon et al. [24]):

$$\ddot{p}_s+2\eta_r\omega_r\dot{p}_s+\omega_r^2 p_s=\xi\omega_r^2 p, \tag{3.1}$$

where p_s is the acoustic pressure in the cavity; p is fluid pressure; ω_r is angular frequency of the resonator and $\omega_r=c\sqrt{A_c/[V(H_c+2H')]}$. A_c is neck section of the cavity, V is volume of the cavity, H_c thickness of the neck of the cavity, H' added thickness (correction) of the neck, η_r is the reduced damping, $\eta_r=\omega^2\omega_r V/(2\pi c^3)$, where ω is angular frequency and V is the volume of the cavity.

The assumption is made that the acoustic wavelength is larger than the geometrical dimensions of the system under consideration, so that the resonator is acoustically compact.

For the corrugated pipe, the instability of the shear layer is strongly influenced by the pipe internal acoustics (Popescu and Johansen [21]). In this case, the driving force (acoustic pressure) in the cavity has the natural frequency of the pipe. Consequently, the acoustic pressure from the neck is replaced by the derivative of acoustic pressure from pipe because, in accordance with Howe's analogy, the acoustic energy generation can be deduced based on the acoustic velocity in the source region (Hirschberg [13]). The Helmholtz resonator neck corresponds to the corrugation and the volume corresponds to the pipe. Since the principal resonator is the pipe, we will interchange the position of ω with ω_r.

The equation that describes the shear instability does not present a self-sustained regime. Hence, we need further modification of Eq. (3.1). We consider a model that was well studied in the dynamical systems literature (Bassand Holster [2] and Gerlach [10]), the van der Pol oscillator, which is a nonlinear oscillator, and, like the cavity in a self-sustained regime, has negative damping at low amplitudes and positive damping at high amplitudes. A way to transform equation (3.1) into a van der Pol type is to replace the reduced damping as follows:

$$\eta_r\rightarrow A\eta_r\left\{\left(\frac{p_s}{B\rho_0U^2}\right)^2-1\right\}. \tag{3.2}$$

As a result, the pressure in the pipe corrugation can be described by the equation:

$$\ddot{p}_s+2\eta_r A\left\{\left(\frac{p_s}{B\rho_0U^2}\right)^2-1\right\}\omega\dot{p}_s+\omega^2 p_s=\xi\omega p', \tag{3.3}$$

where p' is the space derivative of the acoustic pressure in the pipe, and

$$\eta_r=\omega_r^2\omega\frac{V}{2\pi c^3}. \tag{3.4}$$

The excitation term in Eq. (3.3) is defined empirically:

$$\xi=\frac{\omega}{\omega_r}\frac{|p|}{|p+p_s|}. \tag{3.5}$$

The source is the vortex excitation caused by the flow over the corrugation. In our feedback model, this source is represented by self-excited oscillators of the Van der Pol type, with saturation expressed in terms of amplitude. Similar ideas were exploited earlier by Facchinetti at al. [9], who showed that some three dimensional feature of the vortex shedding in the near wake of stationary slender bluff bodies in stationary flows can be described qualitatively and quantitatively by a lower order dynamical model, formed by van der Pol oscillators along the spanwise extent of the structure

$$\frac{\partial^2 q}{\partial t^2}+\varepsilon\omega(q^2-1)\frac{\partial q}{\partial t}+\omega^2 q-\nu\frac{\partial^3 q}{\partial t\partial z^2}=0, \tag{3.6}$$

where z is the direction of the axis of the pipe, q is a dimensionless variable describing the wake flow, ν is a diffusion parameter, ω is the vortex shedding angular frequency and, ε is a positive parameter of the van der Pol oscillator. The authors demonstrated that the diffusion interaction is able to model vortex shedding in shear flow. Taking into account Eqs. (3.3) and (3.6), we obtain the final form of the source equation:

$$\ddot{p}_s+2\eta_r A\left\{\left(\frac{p_s}{B\rho_0 U^2}\right)^2-1\right\}\omega\dot{p}_s+\omega^2 p_s-\nu\frac{\partial^3 p_s}{\partial t\partial z^2}=\xi\omega p'. \tag{3.7}$$

In Eq. (3.7), two coefficients, A and B, need to be prescribed. Next we discuss these two coefficients: A and B.

3.1.1 Coefficient "A"

Tam and Block [29] suggested that the instability of free shear layer has an important contribution to the driving mechanism of cavity oscillation. The unstable behavior of this phenomenon constitutes an essential ingredient in understanding the origin of the pressure oscillations.

Huerre and Monkewitz [16] demonstrated that the mixing layer with a small velocity ratio was subject to connectivity stability. Hémon et al. [12] showed that in case of flow over a cavity, the streamwise direction is bounded by the edges, which leads to perturbations generated by the periodic impingent of the vortices. The strength of these perturbations will determine the generation of the self sustained shear layer oscillations, the frequency of which is related to the distance between the upstream and downstream edges (Popescu and Johansen [21]). For flow over a cavity, the bottom part of the boundary layer develops into a shear layer and the boundary layer vortices may roll up into a discreet vortex (Tietjens [30]). The process is similar to Kelvin-Helmholtz instability (Dommelen [31]).

The dimension of the boundary layer is in this case directly connected to the spatial scale of the shear layer instability, and accordingly, to the thickness of the shear layer. As we know, the shear layer of an oscillating cavity is turbulent. In the instability zone, only a part of the energy associated to the pressure fluctuation is radiated like sound (Roger and Charbonnier [26]). In this flow regime, pressure fluctuations are dominated

by the inertial effect rather than the compressibility. Hence, by increasing the shear layer thickness, the occurrence of lock-in regimes will be prevented. We can conclude that, to be able to have a stronger signal from the source, we need the shear layer to be thinner. Finally, we can notice that the shear layer thickness (in consequence also boundary layer thickness) controls the way in which the sound pressure propagates through system, which is the role of coefficient A in the Van der Poll Eq. (3.7).

The parameter A from the equation that describes the source sound has the same behavior as the thickness of the boundary layer. An approximation of the A parameter should be connected to the thickness of boundary layer. In this work we propose an empirical value for A:

$$A = 0.5^* BLR, \tag{3.8}$$

where BLR is the ratio between the boundary layer thickness and the radius of the pipe. If BLR is close to one, we deal with only turbulent flow. In this case the feedback mechanism doesn't exist, and the singing phenomenon doesn't appear.

3.1.2 Coefficient "B"

Krishnamurty [18] and Rossiter [27] recognized that the interaction between the oscillating shear layer and the trailing edge of the cavity produced intense acoustic disturbances. Experimental evidence confirms the existence of this acoustic source. Heller and Bliss [11] used the water table visualization to observe the sequence of events which took place during a typical oscillation cycle. They found that the compression wave (shock wave) produced at the trailing edge of the cavity extended from inside the cavity all the way to the supersonic outside flow. Before being modified by the outside mean flow, observations clearly indicate that the pressure disturbances inside and outside the cavity are in phase. In consequence, one of main mechanisms controlling the sound pressure level is played out by the interaction between the shear layer and the trailing edge, and the resonance characteristics of the cavity. In consequence, the shape and the volume of the cavity will control the limitation of the pressure field variations. This is the role played by the coefficient "B" in the Van der Pol equation. Unfortunately, we do not yet have a very well defined procedure to obtain the value of parameter B. In this work we choose the empirical value of B as the ratio between the volume of the cavity and the volume of the pipe of length of the cavity opening.

3.2 Acoustic pressure in the pipe

In the pipe, the acoustic behavior can be described as the lossless medium moving with a constant velocity linear wave equation:

$$\begin{cases} \dfrac{\partial(\rho_0 u)}{\partial t} + U\dfrac{\partial(\rho_0 u)}{\partial z} + \dfrac{\partial p}{\partial z} = F(z,t), \\ \dfrac{\partial p}{\partial t} + U\dfrac{\partial p}{\partial z} + \rho_0 c_0^2 \dfrac{\partial u}{\partial z} = 0, \end{cases} \tag{3.9}$$

where the source term from previous equation is

$$F(z,t)=G\frac{\partial p_s}{\partial z}, \tag{3.10}$$

where p_s is the pressure variation caused by the source cavities. G is a constant that depends on the mouth area of the cavity because the feedback mechanism depends on the contact area between flow from to cavity and the flow from pipe (the pipe that has a length equal to the cavity pitch length). We established the empirical value of G is the ratio between width of the cavity and the cavity pitch length.

The acoustic formulation represented by Eq. (3.9) is coupled with N equations for the source variables formulated such that each source oscillates with characteristic frequency ω. The position and the number of the sources are determined by the position and the number of the corrugations in the pipe.

Eqs. (3.7) and (3.9) are solved using high order schemes: Optimized Prefactored Compact finite volume (OPC-fv) scheme (Popescu et al. [22]) for discretization in space, and Low Dissipation and Dispersion Runge-Kutta scheme (Hu et al. [15]) for time stepping. These techniques are designed to handle wave propagation with source terms, and are capable of producing solutions of low numerical dispersion and dissipation, as well as satisfactorily honoring the conservation laws.

3.3 Numerical scheme: space discretization: Optimized Prefactored Compact-Finite Volume (OPC-fv) Scheme

As detailed by Popescu et al. [21–23], consider the first-order, one-dimensional linear wave equation

$$\frac{\partial u}{\partial t}+c\frac{\partial u}{\partial x}=0. \tag{3.11}$$

To derive the discretized equation, we employ the grid point cluster focusing on the grid point i (see Fig. 9), who has the grid points $i-1$ and $i+1$ as its neighbors. The dashed lines define the control volume, and the letters e and w denote the east and west faces, of the control volume, respectively.

To offer a better understanding of the OPC-fv scheme, we first summarize the original finite difference version of the OPC scheme developed by Ashcroft and Zhang [1], termed OPC-fd. The factorized compact scheme in the finite difference approach is obtained by defining the forward and backward operators D_i^F and D_i^B such that

$$\left(\frac{\partial u}{\partial x}\right)_i=\frac{1}{2}\left(D_i^B+D_i^F\right). \tag{3.12}$$

The generic stencils for the 4^{th}-order forward and backward derivative operators are

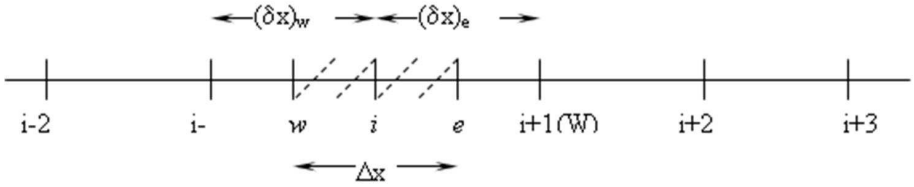

Figure 9: Grid points cluster for one-dimensional problem.

given by

$$\eta_F D^F_{i+1}+\beta_F D^F_i=\frac{1}{\Delta x}\left[a_F u_{i+2}+b_F u_{i+1}+c_F u_i+d_F u_{i-1}+e_F u_{i-2}\right], \tag{3.13a}$$

$$\beta_B D^B_i+\eta_B D^B_{i-1}=\frac{1}{\Delta x}\left[a_B u_{i+2}+b_B u_{i+1}+c_B u_i+d_B u_{i-1}+e_B u_{i-2}\right]. \tag{3.13b}$$

The coefficients are obtained by imposing that: i) the scheme has a certain order of accuracy, and ii) dispersion and dissipation are minimized over a selected window of frequency. As illustrated in Fig. 9, the points i, $i+1$, etc are the nodes where the dependent variables are defined, while e and w define the boundary of a cell centered at point i. The finite volume formulation of the optimized prefactored scheme is obtained by taking into account Eqs. (3.12)-(3.13b), using the idea that the approximation of function at points e and w should have identical forms so that no artificial source/sink is generated. Again, consider a one-dimensional problem with unit thickness in y and z directions

$$\int_e^w \frac{\partial u}{\partial t}dx+c\big((Au)_e-(Au)_w\big)=0, \tag{3.14}$$

where $(Au)_e$ and $(Au)_w$ are the fluxes across the east and west faces, respectively. Hence, the discretized wave Eq. (3.11) can be written as

$$\frac{\partial \overline{u}}{\partial t}\Delta x+c\big((Au)_e-(Au)_w\big)=0, \tag{3.15}$$

where $\overline{u}$ is the averaged value of u over the control volume.

Based on the OPC-fd scheme, the value of the function in the center of the face is defined by the relations

$$\begin{cases} u_e=0.5\big(u^{Fe}+u^{Be}\big), \\ u_w=0.5\big(u^{Fw}+u^{Bw}\big), \end{cases} \tag{3.16}$$

where u^{Fe}, u^{Be}, u^{Fw} and u^{Bw} are determined from

$$\eta u^{Fe}_{i+1}+\beta u^{Fe}_i=bu_{i+1}-du_i, \qquad \eta u^{Fw}_{i+1}+\beta u^{Fw}_i=bu_i-du_{i-1}, \tag{3.17a}$$

$$\beta u^{Be}_i+\eta u^{Be}_{i-1}=bu_i-du_{i+1}, \qquad \beta u^{Bw}_i+\eta u^{Bw}_{i-1}=bu_{i-1}-du_i, \tag{3.17b}$$

and the coefficients are the same as those in the OPC-fd scheme:

$$\begin{cases} \eta=\eta_F=\gamma_B, & \beta=\beta_F=\beta_B, \\ b=b_F=-d_B, & d=d_F=-b_B. \end{cases} \tag{3.18}$$

4 Results and discussion

A main interest of the acoustic simulation of the corrugated pipes is to predict the lock-in behavior and the onset flow rate. We assess the computational outcome by utilizing available field measurements from gas transport systems.

To estimate the frequency that is characteristic of certain cavity geometries and for a certain velocity, we compute Strouhal numbers using computation fluid dynamics around a single cavity with the periodic boundary condition. Experimental measurements for two different pipe and flow configurations are available (Kristiansen and Wiik [19] and Dhainaut [8]) and are used to evaluate the present computational model. Table 2 summarizes the geometric and flow parameters. Figs. 2(a), (b) and (c) show the schematic geometry configurations of the two cases. In all cases the Mach number is less than one.

Table 2: Pipe and flow configurations considered.

Characteristics	Case I	Case II
Pipe internal diameter	2.54×10^{-2}m	3.91×10^{-1}m
Corrugation pitch	5.3×10^{-3}m	2.366×10^{-2}m
Cavity depth	3.11×10^{-3}m	7.66×10^{-3}m
Cavity length	3.12×10^{-3}m	7.76×10^{-3}m
Pipe length	6.15×10^{-1}m	25.0m
Reference density	1.225kg/m^3	100kg/m^3

Case I is based on the previously defined 6.148E-01m pipe and corrugation characteristics are presented in Table 2 and Fig. 2(a). Based on the computation of the flow around a single cavity with periodic boundary condition, and as confirmed by the experimental data, the Strouhal number is approximately 0.61 (see Table 1). In Fig. 10(a), a limit cycle of the source is presented for the fluid velocity of 18m/s. As expected, the limit circle forms after a while when the coupling between acoustics and fluid flow becomes balanced. Fig. 10(b) presents the prediction of the resulting acoustic wave in the pipe for the case of an 18m/s average fluid velocity, caused by the vortex excitation around the cavity. In this case we deal with a self sustained regime, namely, a singing pipe. This figure shows that the amplitude of the acoustic pressure remains constant, which indicates stability of the acoustic system (singing).

The simulation was done for flow between 5.5 and 20m/s, but the singing was observed only for velocity higher than 6m/s. The experimental results recorded indicate that singing starts at a fluid speed of 3.8m/s, which correspond to the one wave length.

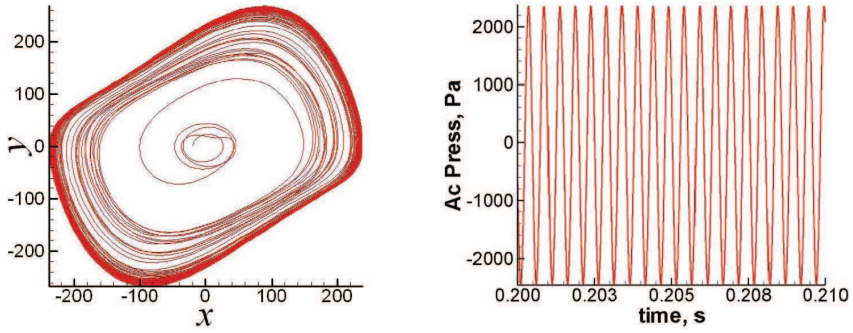

(a) (b)

Figure 10: Numerical simulation of Case I, for $U=18$m/s: (a) Phase plan of the source: limit circle: $x=$ fluid pressure, and $y=$ time derivative of the fluid pressure; (b) Acoustic pressure variation.

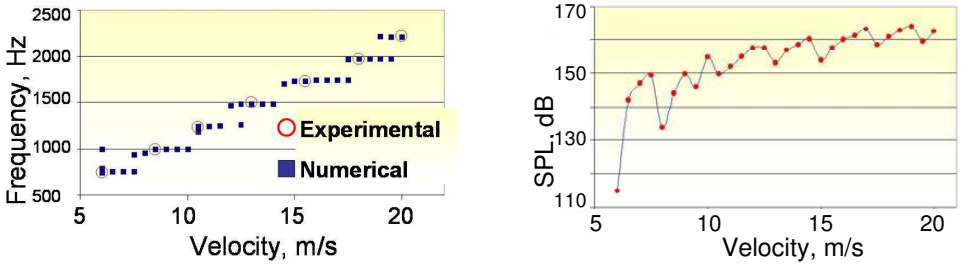

(a) (b)

Figure 11: Case I: (a) Evolution of frequency of acoustic pressure in function of the velocity of the flow; (b) evolution of sound pressure level of the acoustic wave in function of the velocity of the flow.

In other words, the model doesn't capture the capacity of singing if the length of the pipe is not at least equal to one and a half wave length.

Fig. 11(a) shows the overall trend of the oscillating frequency of the system as the velocity is increased. We notice different stages corresponding to the lock-in phenomenon. The various stages are separated by jumps in frequency. The prediction agrees well with the experimental data in all cases, with the maximum error of 1.25%.

In Fig. 11(b) is shown evolution of sound pressure level of the acoustic wave in function of the velocity of the flow. Overall, the higher velocity will induce higher acoustic pressure amplitudes. Locally it is also noticed that the pressure amplitude is characterized by a minimum for the velocity for which the lock-on frequency is changed. In this case the system is characterized by more than one dominant frequency: the system goes through a minimum in energy. This phenomenon was also observed in the experiments done by Debut et al. [7].

The pressure oscillation in the pipe is driven by vortex shedding from the cavity and the shear layer instability. When the shear-layer frequency coincides with a natural frequency of the pipe, the acoustic oscillation of the tube is resonantly excited. The oscillations under discussion are a consequence of a coupled fluid-acoustic system. The acoustic

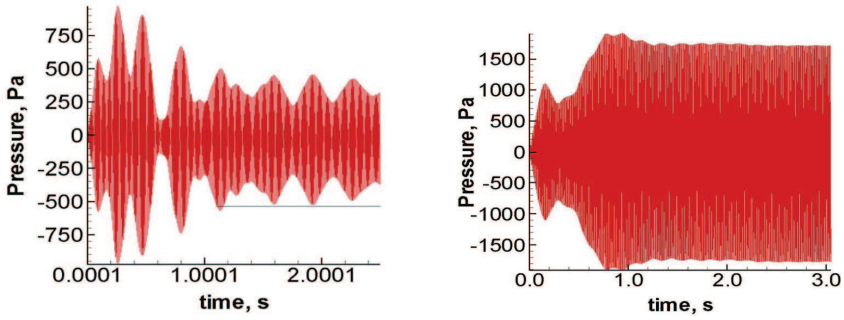

(a) (b)

Figure 12: Numerical simulation of Case II: (a) Acoustic pressure variation for $U=3$m/s; (b) Acoustic pressure variation for $U=3.5$m/s.

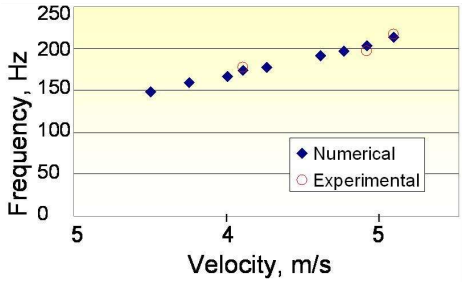

Figure 13: Evolution of frequency versus mean flow velocity in Case II.

field responds to the shear layer instability (local acoustic mechanism) and the geometry of the tube (resonance). The fluid flow is influenced by the acoustic field, while the shear layer frequency is influenced by the acoustic frequency, and adapts to it. Consequently, both acoustic of the pipe and shear layer get in resonance when the lock-on frequency is present and it appears only one dominant frequency over a range of fluid speeds. When these two subsystems do not get in resonance, we deal with more than one frequency; in this case the system tends towards a minimum in total energy.

In Case II we apply the model to a 25m long pipe that has a corrugation geometry that is presented in the Fig. 2(b) and (c): the pipe and corrugation characteristics are presented in Table 2. The simulations were done for the fluid velocity ranging from 3m/s to 5m/s. The Strouhal number based on the flow around of a single cavity is approximately equal to one. As shown in Fig. 12(a), for a fluid velocity of 3m/s, the acoustic wave decays in time, indicating that singing cannot be sustained at this velocity. In fact, singing is not attained computationally for a fluid velocity lower than 3.5m/s. Fig. 12(b) shows the simulation for a fluid velocity equal to 3.5m/s. In this case the amplitude of the acoustic pressure will not decay, but it is constant. In consequence, the singing is obtained for a value of the velocity larger or equal to 3.5m/s. In consequence, this is the predicted on set velocity. This predicted value is the same as that reported in the experimental data (Dhainaut [5]). Fig. 13 shows the general trends of the oscillating frequency of the

system versus the fluid velocity. The numerical simulation and the experimental data again agree with each other favourably.

5 Summary and conclusions

In this work we have developed a one dimensional flow-acoustics model, which couples the vortex shedding mechanism and the acoustic oscillation in a corrugated pipe. The model consists of two key components: (i) an acoustic treatment, assuming a lossless medium where the fluid flow is modeled as a perturbation of a constant velocity, represented by a linear wave equation; (ii) an oscillator model, based on the Van der Pol type equation, which takes into account the vortex shedding in shear flow and excitation and damping according to the shear layer instability theory.

The model was validated against two experimental cases. The solution demonstrates that the model can capture the capacity of singing only for pipes longer than 1.5 wave lengths of the acoustic wave. Furthermore, the model is capable of predicting the lock-on frequency as well as the onset fluid velocity.

It was revealed that the frequency of the impinging-shear-layer instability increases with the average flow velocity. However, the strict proportionality is observed only in the case of computation of flow around a single cavity, with periodic boundary conditions and where the feedback mechanism is not present.

The maximum shear layer instability is found in the regions with maximum acoustic pressure variations, which indicates that the fluid system is powerfully influenced by the acoustic subsystem. This illustrates the importance of taking into consideration the interaction between flow and acoustics. In conclusion, corrugated pipes are predisposed to singing if the feedback mechanism determines that the waves have a certain level of amplitude.

The acoustic wave that appears in the open corrugated tube is characterized by natural harmonics of the tube which is excited by the instability of the impinging-shear-layer that appears in the flow over the corrugations. It is also noted that overall *increasing velocity induces higher acoustic pressure*. However, the pressure drops to a minimum when the lock-on frequency is changed as the acoustic system goes though a minimum energy.

Nomenclature

A, B, ξ, α	constants
A_c	neck section of the cavity
BLR	boundary layer thickness
c	speed of sound
dt	time step
dx	grid size in space
H'	added thickness

H_c	thickness of the neck
L	pitch length
M	Mach number
p	acoustic pressure of the pipe
p_n	pressure in the neck of the cavity
p_s	source pressure
q	dimensionless variable
St	Strouhal number
t	time
U	average flow velocity in the pipe
u	acoustic velocity
V	volume of the cavity
z	axial coordinate of computation domain
η_r	the reduced damping
ν	kinematics viscosity
ρ_0	reference density
ω	frequency
ω_r	angular frequency of the resonator

Acknowledgments

The work was funded by the Norwegian Research Council, together with the industrial partners Wellstream, Technip and StatoilHydro. Special thanks go to project manager Øyvind Hellan for the support given during this work.

References

[1] G. Ashcroft and X. Zhang, Optimized prefactored compact scheme, J. Comput. Phys., 190 (2003), 459–477.
[2] R. L. Bass and J. L. Holster, Bellows vibration with internal cryogenic flows, ASME J. Eng. Ind., 91(1) (1972), 70–75.
[3] L. H. Cadwell, Singing corrugated pipes, Am. J. Phys., 62(3) (1994), 224–227.
[4] T. Colonius, A. J. Basu and C. W. Rowley, Numerical investigation of the flow past a cavity, AIAA Paper No. 99-1912, 5th Aiaa/CEAS Aeronautics Conference, May 1999.
[5] F. S. Crawford, Singing corrugated pipes, Am. J. Phys., 42 (1974), 278–288.
[6] V. Debut, J. Antunes and M. Moreira, A phenomenological model for sound generation in corrugated pipes, ISMA, 2007.
[7] V. Debut, J. Antunes and M. Moreira, Experimental Study of the Flow-Excited Acoustical Lock-In in a Corrugated Pipe, ICSV14, Cairns, Australia, 2007b.
[8] M. Dhainaut, CFD Modelling Activity for the Singing Riser Project-part II: Real Case Simulation SINTEF, Singing riser 805016, Trondheim, 2005.
[9] M. I. Facchinetti, de E. Langre and Biolley, Vortex shedding modeling using diffusive van der Pol oscillators, Mécanique des Fluides, Série IIb, (2002), 1–6.

[10] C. R. Gerlach, Vortex excitation of metal bellows, J. Eng. Indust., 94(1) (1972), 87–94.
[11] H. H. Heller and D. B. Bliss, The physical mechanism of flow induced pressure fluctuations in cavities and concepts for their suppression, AIAA Paper No. 75-491, 1975.
[12] P. Hémon, F. Santi and X. Amandolèse, On the pressure oscillation inside a deep cavity excited by a grazing airflow, Euro. J. Mech. B. Fluids., 23 (2004), 617–632.
[13] A. Hirschberg, Aeroacoustics of wind instruments, in Mechanics of Musical Instruments CISM Courses and Lectures, Springer-Verlag, 1995.
[14] M. S. Howe, Mechanism of sound generation by low Mach number flow over a wall cavity, J. Sound. Vibrat., 73 (2004), 103–123.
[15] F. Q. Hu, M. Y. Hussaini and J. Manthey, Low dissipation and dispersion Runge-Kutta for computational acoustics, J. Comput. Phys., 124 (1996), 177–191.
[16] P. Huerre and P. A. Monkewitz, Absolute and convective instability of the hyperbolic-tangent velocity profile, J. Fluid. Mech., 159 (1985), 151–168.
[17] E. Klaeui, Jet: vibration tests on calorimeter bellows, Report No. 3554/1512, Sulzer Bros. Ltd., Winterthur, Switzerland, 1987.
[18] K. Krishnamurty, Acoustic radiation from two-dimensional rectangular cutouts in aerodynamic surface, N.A.C.A. Tech. Note., No. 3487, 1955.
[19] U. R. Kristiansen and G. A. Wiik, Experiments on sound generation in corrugated pipe with flow, J. Acoust. Soc. Am., 121(3) (2007), 1337–1344.
[20] Y. Nakamura and N. Fukamachi, Sound generation in corrugated tubes, Fluid. Dyn. Res., North Holland, 7 (1991), 255–261.
[21] M. Popescu and S. T. Johansen, Acoustic wave propagation in low Mach flow pipe, AIAA Paper No. 08-95691, 46th AIAA Aerospace Sciences Meeting and Exhibit, 2008.
[22] M. Popescu, W. Shyy and M. Garbey, A study of dispersion-relation-preserving and optimized prefactored compact schemes for wave equation, J. Comput. Phys., 210(5) (2005), 705–729.
[23] M. Popescu, R. Vedder and W. Shyy, A finite volume-based high order, Cartesian cut-cell method for wave propagation, Int. J. Numer. Methods. Fluids., 56 (2008), 1787–1818.
[24] T. A. Reinen, Singing riser: overwie, SINTEF, Singing riser 805016, Trondheim, 2007.
[25] D. Rockwell and A. Schachenmann, The organized shear layer due to oscillations of a turbulent jet through an axisymmetric cavity, J. Sound. Vibrat., 87 (1983), 371–382.
[26] M. Roger and J. M. Charbonnier, Applied aero-acoustics: prediction methods von Karman institute for fluid dynamics, Lecture Series, 1996-04, 1996.
[27] J. E. Rossiter, Wind-tunnel experiments on the flow over rectangular cavities at subsonic and transonic speed, Technical Report 3438, Aeronautical Research Council Reports and Memoranda, 1964.
[28] C. W. Rowley and D. R. Williams, Dynamic and control of high Reynolds number flow over open cavities, Annu. Rev. Fluid. Mech., 38 (2006), 251–276.
[29] C. K. W. Tam and P. J. W. Block, On the tones and pressure oscillations induced by the flow over rectangular cavities, J. Fluid. Mech., 89 (1978), 373–399.
[30] O. Tietjens, Strömungslehre, 1st Ed., Springer-Verlag, Berlin, (1970), 105–109.
[31] L. L. van Dommelen, Unsteady Boundary Layer Separation, Ph.D. thesis, Cornell University, 1981 (unpublished).
[32] D. S. Weave and P. Ainsworth, Flow induced vibration in bellows, International Symposium on Flow-Induced Vibration and Noise, Chicago, (1998), 205–214.
[33] S. Ziada, M. Eng, M. Asme and E. T. Buhlmann, Flow induced vibration in long corrugated pipes, C416/010@IMechE, (1991), 417–426.